Proceedings of ASME Turbo Expo 2022
Turbomachinery Technical Conference and Exposition
GT2022
June 13-17, 2022, Rotterdam, The Netherlands

GT2022-79399

SIMULATION OF A SAFE START-UP MANEUVER FOR A BRAYTON HEAT PUMP

Johannes Oehler[1]*, **A. Phong Tran**[1], **Panagiotis Stathopoulos**[1]
[1]German Aerospace Center (DLR), Institute of Low-Carbon Industrial Processes, Cottbus, Brandenburg, Germany

ABSTRACT

With about 50 % of the final energy used as heat in Europe, reducing fossil fuel consumption in this sector is crucial to achieve significant greenhouse gas emission reduction. Heat pumps using renewable electricity can potentially cover the heat demand below 500 °C.

The DLR's prototype CoBra (Cottbus Brayton cycle heat pump) aims at demonstrating the feasibility of a turbomachine driven closed-loop Brayton cycle heat pump with a thermal output of 200 kW and a heat sink temperature of up to 350 °C. In order to achieve safe operation, transient operation of the heat pump, such as start-up, must be analyzed. Temperature gradients must be kept below a limit, defined mostly by thermal stresses in the heat exchangers. At the same time, compressor surge and resonant frequencies of rotating components must be avoided during transient maneuvers of the system.

In the current work, the heat pump prototype has been modeled with Modelica based on the component geometries and with the use of compressor and turbine maps obtained from 3D CFD simulations. For the start-up of the prototype, a suitable control strategy is developed and analyzed in order to minimize operational risks. Control parameters are compressor shaft speed, secondary mass flows and the turbine bypass.

It is shown that a turbine bypass is necessary to avoid compressor surge during start-up. The conflicting requirements of crossing natural frequencies quickly while ensuring tolerable temperature gradients in the heat exchangers can be met. The results also show that pressure rise delay through volume dynamics is in the order of seconds. Slow transient effects in the evolution of fluid and heat exchanger temperatures arise from the thermal inertia of the heat exchangers.

*Address all correspondence to johannes.oehler@dlr.de

Keywords: high temperature heat pump, reverse Brayton cycle, process heat, Modelica, transient process simulation

NOMENCLATURE

CFD	computational fluid dynamics
CoBra	Cottbus Brayton cycle heat pump
COP	coefficient of performance
DLR	German Aerospace Center
HTHE	high-temperature heat exchanger
LTHE	low-temperature heat exchanger
MSL	Modelica Standard Library
EO	engine order
f_c	compressor shaft speed
f_n	natural frequency
$f_{off-limit}$	rotational frequency with possible resonance
$\dot{m}_{red}$	reduced mass flow (normalized to International Standard Atmosphere conditions)
p	pressure
Π_c	compressor total pressure ratio
q_h	useful high temperature heat
q_w	utilized waste heat
T	temperature
$\bar{T}_c$	mean temperature of compression
$\bar{T}_t$	mean temperature of expansion
t	time
w	work performed in the Brayton cycle

1 Introduction

Half of the final energy consumed in Europe is used for providing heat [1]. This energy mainly stems from fossil sources today [2] which leads to the current dangerous and unprecedented increase in earth's temperature [3]. In order to reduce global warming, this energy demand must be met with emission-free technology. Heat pumps, driven with renewable electricity, offer a viable and efficient possibility. For cooling and low-temperature applications such as heating and warm water, the technology is readily available. For industrial applications beyond 100 °C, there are few operational machines; the current limit for industrial heat pumps is 150 °C sink temperature [4]. Nevertheless using heat pumps to provide higher temperatures is a promising option in chemical, paper or food industries [5]. The limitation of traditional working fluids with their critical point at 200 °C or below can be overcome by using a reverse Brayton cycle heat pump. The Brayton cycle known from gas turbines is operated without phase transition, hence there is no upper temperature limit from the condensation temperature of the working medium.

The Brayton cycle has been proposed for both heat pumps and heat engines in pumped thermal energy storage systems [6, 7]. McTigue et al. [6] claim that round trip efficiencies as high as 70 % are feasible for such a system. The Cottbus Brayton cycle heat pump CoBra is intended only for heat pump operation and shall operate in a closed cycle. It will be the first Brayton cycle high temperature heat pump that supplies heat above 250 °C and the first turbomachine-driven Brayton heat pump with more than 200 kW thermal power.

Transient models of Brayton systems for power or heat conversion have been developed using tools such as Modelica [8], TRNSYS [9] or GT-SUITE [10]. Recently, the simulation of closed-loop Brayton cycles using supercritical carbon dioxide has received attention [11, 12]. A wide range of Modelica libraries for modeling thermo-fluid systems are available, including the open-source libraries ThermoPower [13], Thermofluid Stream [14] and ThermoSysPro [15]. ThermoPower's modeling capabilities have been demonstrated, e.g., for the simulation of start-up processes of combined cycle power plants [16] or coal-fired power units [17].

Just as for gas turbine operation, the compressor stability, temperature gradients and resonance frequencies of the fast rotating turbomachines must be considered for safe operation of the heat pump. Since the start-up spans over the whole range of rotational frequencies and temperatures and is logically the first maneuver to perform, we chose to model and analyze the start-up from standstill until nominal full power operation. Due to the technical novelty of closed-loop Brayton heat pumps, the present work marks the first investigation of the start-up process of this heat pump type.

2 Prototype and problem description

At the DLR Institute of Low-Carbon Industrial Processes, a prototype of a Brayton cycle high-temperature heat pump is developed and tested. For safety reasons and because of the availability of suitable compressors, air is used as a working medium. The concept can be seen in Fig. 1. The prototype mainly consists of a compressor, a turbine and three shell-and-tube heat exchangers, of which one is the recuperator. Numbers 1 through 4 correspond to the system states at turbomachine inlets and outlets. Compressor and turbine are mounted on two independent shafts for more experimental freedom and each is coupled with an electric machine through a gearbox. The three-stage compressor, used in the heat pump, has been derived from a turboshaft engine, originally designed for unmanned helicopters [18]. More detail on the components and their modeling is given in Section 3.

The heat pump compresses the working medium in the compressor (intake is state 1 in Fig. 1), then rejects the heat in the high temperature heat exchanger (HTHE) and expands the gas stream in the turbine. The loop is closed by heating the cold gas stream after the turbine, employing the low temperature heat exchanger (LTHE) taking heat from ambient air or a waste heat stream. Since the mean temperature regime of the expansion $\bar{T}_t = 40\,°\mathrm{C}$ is lower than that of compression $\bar{T}_c = 150\,°\mathrm{C}$, a positive net work w must be supplied to the primary cycle from the electricity grid (see Fig. 1). Since the turbine work is used to drive the compressor this net work is the difference between compressor work W_c and turbine work W_t (see Eq. 1). The heat output at the high temperature side however can be larger than the electric power input because of the absorbed ambient heat, which is lifted to higher temperatures. The ratio of useful heat to net work is generally described as the coefficient of performance COP in Eq. 1.

$$COP_{\text{heating}} = \frac{q_h}{w} = \frac{q_h}{w_c - w_t} \tag{1}$$

With any value of $COP > 1.0$, the machine is more efficient than direct electrical heating. For low temperature applications, such as space heating, values as high as $COP = 4$ are possible. High temperature heat pumps with large temperature differences operate at considerably lower COPs. For the CoBra prototype, the calculated COP value for nominal operation is $COP_{\text{CoBra,nominal}} = 1.48$ for an output temperature of 276.9 °C (550 K) using only ambient air with 15 °C as heat source [19].

3 Transient heat pump modeling methodology

The transient model of the CoBra heat pump is implemented using the modeling language MODELICA [8] due to its suitability for multi-domain and complex systems. SIMULATIONX [20], developed by ESI ITI, is used as the modeling environment.

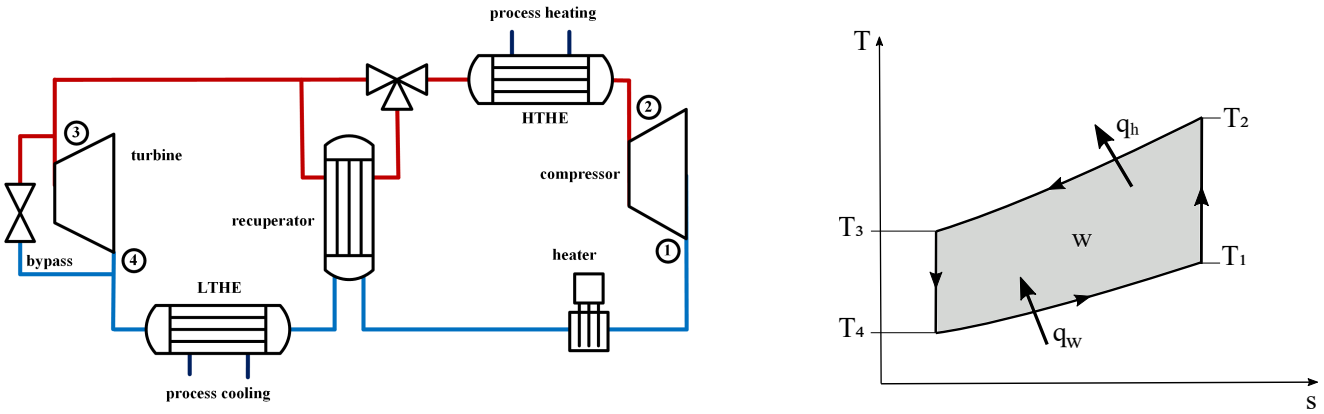

FIGURE 1. Schematic of the CoBra prototype (left) and equivalent thermodynamic cycle

The component models from the ThermoPower library [13] are reused to model the heat pump components. ThermoPower provides basic components for system-level modeling of power plants and energy conversion systems. Since ThermoPower is compatible with the interfaces defined in the Modelica Standard Library (MSL), the transient model also incorporates MSL models, in particular from the Thermal, Media and Mechanics sublibraries. The used components are connected with each other following the actual process schematic (see Fig. 1), thereby creating a system of equations that models the behavior of the heat pump system.

Turbomachinery The compressor and turbine models of the ThermoPower library are modeled through performance maps, which are obtained from 3D CFD simulations. The performance maps do not model turbomachine-intrinsic dynamics, which occur at significantly smaller time scales compared to volume and thermal inertia. Both turbocomponents are connected with their respective shaft inertia through a mechanical connector. When simulating the model, either torque or shaft speed can be specified.

Heat Exchangers The three shell-and-tube heat exchangers are custom-built by Apparate- und Anlagentechnik Nuernberg GmbH. They are modeled using ThermoPower's one-dimensional finite volume flow and thermal models. Each heat exchanger flow side is represented by a 1D pipe flow model approximating the actual flow regime and surface geometry. Both sides' flow model volumes are connected with counter-current mapping to one another, matching the heat exchanger's flow configuration. The heat transfer coefficients for a nominal operating point are taken from manufacturer data and scaled for different mass flow rates. Thermal inertia is modeled by placing heat capacities in between the two flow models via finite volume thermal models representing tubes and shell of the heat exchanger. The flow and thermal models are discretized into four and three volumes, respectively. Mass, momentum and energy balance equations are applied for the flow models.

Piping Pipes contribute significantly to the total system volume and are therefore modeled as adiabatic, lumped volumes based on the actual pipe section geometries.

Valves The turbine bypass valve and the recuperation three-way valve (see Fig. 1) are considered in the transient model. In the gas valve model of ThermoPower, the flow characteristic consisting of K_v value and characteristic type needs to be specified. Both parameters can be taken from manufacturer data. All modeled valves possess linear flow characteristics. The three-way valve is composed of two inversely linked valves, such that opening one valve results in closing of the other.

Heater The heater upstream of the compressor is modeled as a lumped volume with an additional thermal port allowing for the influx of heat. A feedback controller (PID) sets the heat flow rate based on the actual compressor inlet temperature T_1 and the target temperature. The heat flow rate is limited to positive values, thus preventing cooling by the heater. The purpose of the heater is simulation of an industrial waste heat source. In this study for start-up the heater was not used.

Model interfaces Taking advantage of Modelica's modular approach, the heat pump model is encapsulated and incorporated in simulation models that provide maneuver data to the heat pump model. The maneuver data is composed of real-value time signals for the following model variables:

- HTHE: Secondary side mass flow rate in kg/s
- LTHE: Secondary side mass flow rate in kg/s
- Compressor shaft flange: Shaft speed in rad/s
- Turbine shaft flange: Shaft speed in rad/s
- Bypass valve: Dimensionless position

- Recuperation three-way valve: Dimensionless position
- Heater: Target temperature in K

In this study, the input signals are supplied from timetables. In addition to this, the initial pressure levels of the heat pump's low and high pressure parts must be specified as parameters. After simulating a maneuver, all computed result variables are available for post-processing, including all flow state variables, metal temperatures and turbomachinery operating points.

4 Simulation boundary conditions and goals

Starting up the heat pump, natural frequencies must be avoided and the temperature gradient, experienced by the heat exchangers, must be limited. The manufacturer of the shell-and-tube heat exchangers recommends a temperature gradient of no more than $2\,\frac{K}{min}$. Additionally, sudden temperature changes should be limited to a maximum of 10 K.

4.1 Natural frequencies of rotating components

Natural frequencies and rotational speeds must be considered for safe operation of turbomachines. The turbine shaft speed can be chosen freely by the generator with only minor effects on the turbine efficiency over a large range of speeds and no relevant effect on the total thermodynamic cycle. The critical areas where natural frequencies and possible resonance occur can therefore be avoided easily. This is why focus is laid on the compressor, where any change of shaft speed has direct effects on the heat pump temperatures and pressures. Thus, critical shaft speed areas cannot be easily avoided. In Fig. 2, the natural frequencies of the compressor shaft are illustrated. The red dashed line shows the maximum shaft speed of $f_{\mathrm{c,max}} = 105\,000$ rpm. The red diagonal operation line is engine order 1 (EO1) and links the shaft speed on the x-axis with the natural frequencies on the y-axis. Four black lines show the first natural frequencies of the shaft. They were calculated by the manufacturer of the compressor and will be experimentally verified upon the first test of the compressor. Natural frequencies f_{n} can be linked to a blocked operational area extending above and below $f_{\mathrm{off-limit}}$, using the Campbell diagram. Red circles mark crossings of engine order EO1 with a natural frequency where resonance is likely to occur. Focus lies on the first two modes since they cross EO1 in the operational range. The third one is a torsion only mode and considered less harmful. The topmost line lies out of the operational range of the compressor.

In addition to the compressor shaft, also its rotor blades possess natural frequencies. Because of their small dimensions and mass and high stiffness, their eigenmodes lie at high frequencies two times or more above the nominal shaft speed. The blades of the first rotor stage are tallest, less stiff and therefore have lower natural frequencies than the later rotor stages. Before the first rotor stage, there are four equally spaced struts that can cause excitation of engine order EO4 of the rotor blades. Therefore only the first rotor stage possesses a natural frequency that crosses with relevant engine orders. In Fig. 3, the Campbell diagram for the first rotor stage with engine orders EO1-8 and EO13 is shown, since the first rotor stage has 13 blades. EO13 excitation is observable with vibration sensors on the compressor casing in experiments, but EO1-4 are dominant.

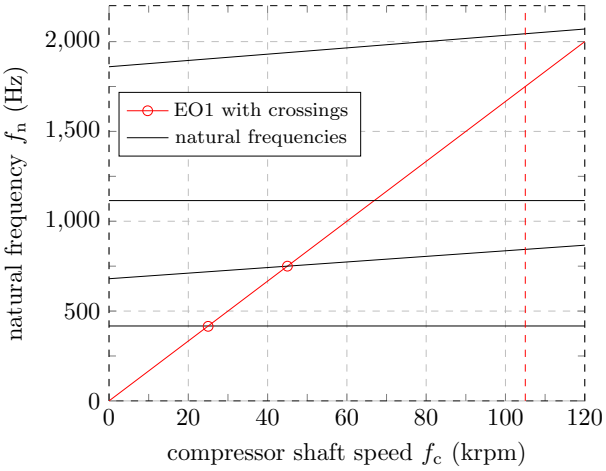

FIGURE 2. Campbell diagram of the compressor shaft

To confirm the calculated natural frequencies of the first rotor stage, they were experimentally determined before assembly and operation. An experimental modal analysis has been conducted by the Chair of Structural Mechanics and Vehicle Vibrational Technology of the Brandenburg Technical University (BTU). The rotor was excited by a miniature impulse hammer and vibrations were measured via laser Doppler vibrometry (see Fig. 4). The excitable frequencies were found to be limited to the range $f_{\mathrm{n,rotor1}} = [3227.5\,\mathrm{Hz}, 3323.3\,\mathrm{Hz}]$ in the absence of any rotor movement. This confirms the calculated natural frequency of the first rotor stage. The natural frequency lies higher in operation when the shaft is turning due to centrifugal forces. This can be seen by the ascending trend of the natural frequency for high rpm in Fig. 3. The speed range for the compressor of $f_{\mathrm{off-limit}} = [54\,000\,\mathrm{rpm}, 56\,000\,\mathrm{rpm}]$ is defined "off-limits" for constant operation, allowing for a safety interval extending over the expected resonance frequencies.

Knowledge of the size of this frequency band and its position is essential to maximize the size of the permitted operational range of the compressor. However, crossing these rotational speed regimes quickly contradicts the requirement for slow temperature gradients. Thus, one major goal of the simulation study is analyzing the effect of quick increases of compressor shaft speed in areas where eigenmodes lie on the temperature rise at the compressor outlet.

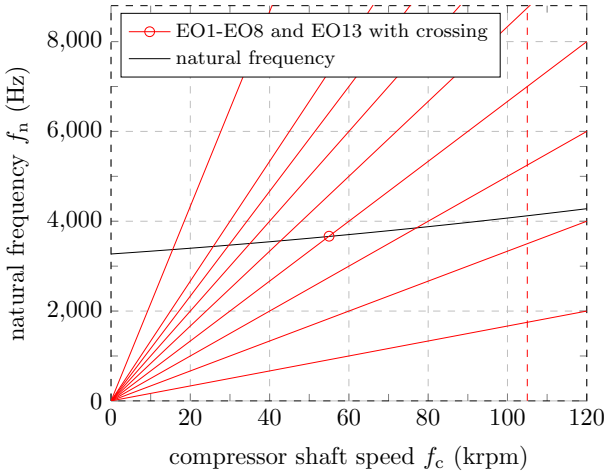

FIGURE 3. Campbell diagram of the first rotor stage of the compressor

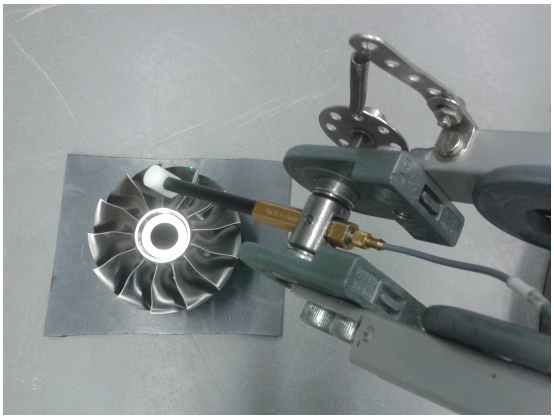

FIGURE 4. Experimental setup for experimental analysis of the blisk rotor's natural frequencies

4.2 Transient start-up simulation

The model outlined in Section 3 is used for investigation of the transient system behavior during the start-up maneuver. Fluid and metal temperatures in the heat pump model are set to an initial value of 15 °C. Furthermore, the pressures are set to starting values of $p_{1,\text{start}} = 3.3\,\text{bar}$ at the low pressure side and $p_{2,\text{start}} = 3.31\,\text{bar}$ at the high pressure side. The small pressure difference is included to support the initialization of the simulation.

Figure 5 shows the main control signals of the start-up maneuver. Compressor shaft speed, turbine bypass valve position and secondary mass flow rates have been selected as the main actuator signals for the start-up process. The slopes of the compressor shaft speed ramps are selected such that the increase in temperature does not exceed 2 K/min. In order to avoid excitation of the natural frequencies identified in section 4.1, the defined blocked speed regimes are traversed with rapid acceleration maneuvers (see red circles in Fig. 5). Heat extraction via the HTHE is initialized after passing the first two critical natural frequencies by starting up the secondary side mass flow. After passing the rotor eigenmode at a compressor shaft speed of $f_{\text{off-limit}} = 55\,000$ rpm, the bypass valve is partially closed, thereby throttling the compressor. A hold time is added to allow observation of the compressor operating point and stabilization of temperatures and pressures. After that, the compressor shaft speed is steadily increased until a speed of 100 % is reached. During acceleration, the bypass valve is gradually closed to avoid operating the compressor in the choke regime. After $t = 2.5\,\text{h}$, the control inputs stay constant until the end of the simulation at $t = 3.0\,\text{h}$. The remaining actuators, i.e., the three-way valve and the heater, are not used in this work.

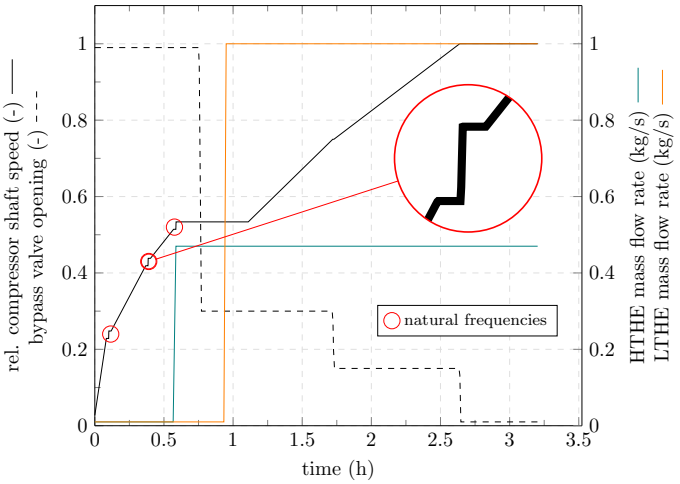

FIGURE 5. Control signals of the start-up sequence

The selected initial and boundary conditions, combined with the system model outlined in Section 3, result in an initial value problem that is solved numerically using the variable-step solver CVODE [21].

5 Results and discussion

5.1 Results

Figure 6 plots the compressor pressure ratio Π_c with surge line and speed lines over the reduced mass flow $\dot{m}_{\text{red}}$ of the compressor. The transient compressor operating line, resulting from the proposed start-up maneuver, is shown in red. The operating line follows the speed lines on three occasions, this corresponds to the three throttling maneuvers shown in Fig. 5, where the bypass valve is being closed. The simulation is ended after three hours with closed bypass valve at the nominal shaft speed of $f_{\text{c,max}} = 105\,000$ rpm and the design pressure ratio of $\Pi_c = 6.15$.

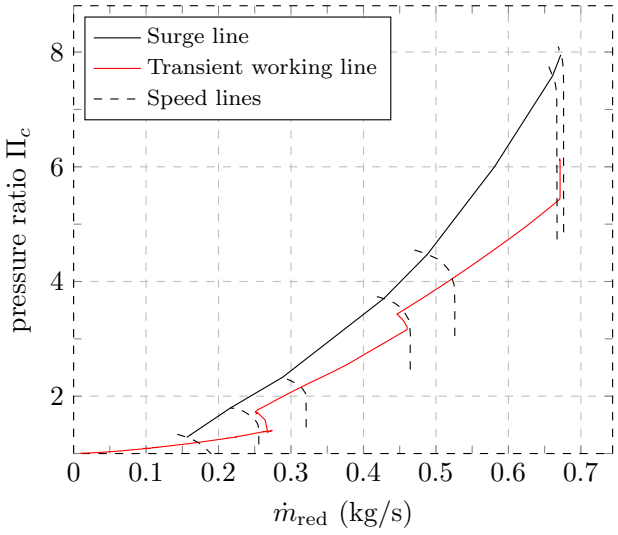

FIGURE 6. Compressor map with transient working line

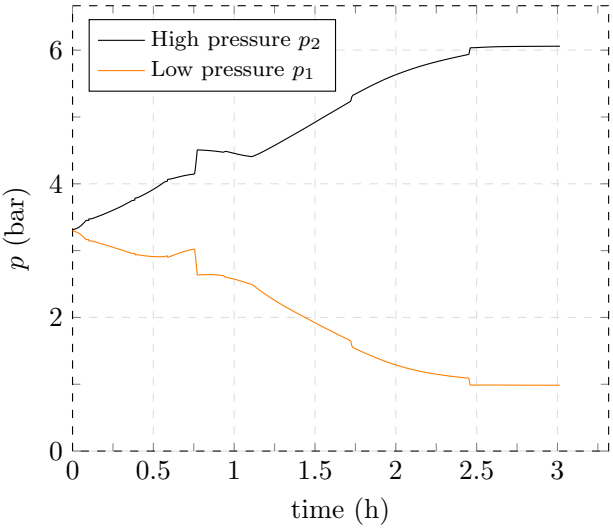

FIGURE 8. Heat pump system pressures

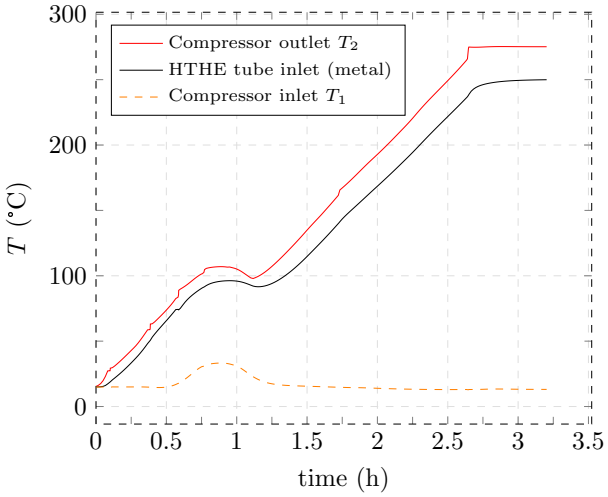

FIGURE 7. Compressor air and HTHE metal temperatures

Figure 7 shows the temperature trends of the compressor inlet and compressor outlet air flow, as well as the metal temperature of the first part of the HTHE. All temperatures start at 15 °C, the hot areas of the compressor outlet and the high temperature heat exchanger inlet leveling out at around 250 °C after three hours of operation.

Figure 8 shows the pressures in the high pressure side (red area in Fig. 1) and the low pressure side (blue area in Fig. 1) that develop in the system during the start-up. Starting from the initial system pressure of $p_{2,\mathrm{start}} = 3.31\,\mathrm{bar}$, the pressures diverge with increasing compressor shaft speed and throttling. The bypass closing maneuvers are evident as pressure ramps.

5.2 Discussion

Figure 6 shows that throughout the start-up maneuver compressor surge can be prevented. However, at part load conditions and a low pressure ratio of around $\Pi_c = 2.0$, the surge margin is small, even with the bypass valve 30 % open. Operating the system without bypass valve would lead the compressor to surge. Therefore, the bypass valve is essential for safe operation, starting the heat pump and transitioning into nominal operation. At higher speeds, closing of the bypass valve is necessary to avoid the choke area of the compressor map. Throttling also increases the efficiency, which can be seen for the throttling maneuver at $t = 1.75\,\mathrm{h}$. During the maneuver the pressure ratio Π increases substantially (see Fig. 8), whereas compressor outlet temperature T_2 increases only marginally (see Fig. 7). Also, the operation point moves closer to the surge line, near which the operational regime with maximum efficiency lies.

The compressor outlet temperature T_2 in Fig. 7 stays just below the maximum allowed slope of $2\,\frac{K}{min}$ throughout the start-up maneuver. During quick changes of shaft speed and bypass valve position, no sudden temperature increase of more than 10 K occurs. The metal temperature of the HTHE rises slower than the compressor outlet temperature and irregularities are generally dampened. This can be best observed at occasions where shaft speed or throttling ratio is suddenly changed. The black line in Fig. 7 does not follow the abrupt variations of the compressor outlet temperature in red. Only after activation of the secondary mass flow in the HTHE, a drop of a few degrees C in the heat exchanger metal temperature can be observed. Generally, the temperature dynamics are slow. This can be observed in the compressor inlet temperature T_1. At the beginning of the maneuver, all heat produced in the compressor is absorbed in the HTHE and LTHE, both of which heat up. Only after $t = 0.5\,\mathrm{h}$,

when also the LTHE temperature is elevated, the compressor inlet temperature starts to rise. After activation of the HTHE mass flow at $t = 0.58\,\mathrm{h}$, which takes away heat from the HTHE and the primary cycle, compressor inlet temperature still increases and peaks at around $t = 0.9\,\mathrm{h}$ at $T_1 = 35\,^{\circ}\mathrm{C}$. The throttling maneuver at $t = 0.8\,\mathrm{h}$ leads to a slight increase of compressor outlet temperature but also to more energy extracted from the primary cycle by the turbine. Consequently, the LTHE temperature decreases and finally the compressor inlet temperature starts to sink again. It takes over half an hour from the activation of HTHE flow until all temperatures stabilize and more than half an hour from the throttling maneuver until the compressor inlet temperature returns to a value of 15 °C. This large time scale can be explained by the thermal inertia of the heat exchangers. The same trend holds at the end of the simulation where HTHE metal temperature levels out only at $t = 3.0\,\mathrm{h}$ although control inputs stay constant from $t = 2.5\,\mathrm{h}$ until the end of the simulation.

The system pressures respond quickly to new control inputs with a time delay of a few seconds. At the absence of new control inputs, the pressures stay constant, which can be observed at the end of the simulated maneuver. This does not hold for the time interval from $t = 0.58\,\mathrm{h}$ until $t = 1.11\,\mathrm{h}$, where only one change in control parameters happens. The turbine bypass valve is closed from open position to 30 % opened at $t = 0.75\,\mathrm{h}$, other control parameters stay constant throughout the time interval. Figure 8 still shows relevant changes in both pressures. At first, both pressures rise. After the effect of the throttling maneuver, both pressures stay constant for a while and then decrease. The transient model is able to predict this first rise of both pressures, which stems from thermal effects. In the interval from $t = [0.6\,\mathrm{h}, 0.75\,\mathrm{h}]$, both pressures increase despite constant shaft speed and valve position, as there is a net heat input into the heat pump system, thus, heating up the fluid in the closed cycle and increasing the pressure level. This characteristic stems from the closed-loop design of the heat pump where the amount of working fluid remains constant, and therefore average pressure and temperature are coupled via the underlying gas model.

5.3 Outlook

The large thermal inertia of the heat exchangers is an issue that hampers quick changes of operation point. Further simulative and experimental work will be conducted to minimize start-up and shut-down times and to evaluate which heat exchanger type and design is best suited for fast load changes. As long as the heat exchangers absorb heat, the heat pump is in a transient mode. Gradual saturation of the HTHE leads to ascending turbine inlet temperatures and can be compared to thermal throttling of the turbine, analog to increased fuel injection in gas turbines. This effect will also be relevant for shut-down of the heat pump, where HTHE temperatures can be higher than the compressor outlet and the HTHE can therefore act as a temperature source instead of a sink.

6 Conclusion

A suitable strategy for start-up of the heat pump prototype CoBra has been proposed. It includes quick traverses of the compressor's natural frequencies and opening of the turbine bypass valve at part load operation. The bypass is closed and the compressor is gradually throttled at higher compressor speeds. The compressor stability can be guaranteed under all load conditions. The simulation of the transient start-up maneuver shows that the conflicting requirements of increasing rotational speed quickly, to avoid vibrational resonance, and increasing temperature slowly, to avoid thermal tensions, can be respected at the same time. Pressure transient effects for filling up volumes, such as heat exchangers and pipes, are in the order of seconds. Temperature transient effects for heating up the metal structure of the heat exchangers are in the order of half an hour. Both system temperature level and pressure level are coupled via the constant fluid inventory in the primary cycle. The modeling of transient effects will be continued in order to study the operational behavior of the heat pump during load change, shutdown and in case of component malfunction.

ACKNOWLEDGMENT

We would like to express our gratitude to AeroDesignWorks for providing extensive data on their compressor and the Chair of Structural Mechanics and Vehicle Vibrational Technology of the Brandenburg University of Technology (BTU) for conducting vibrational tests and providing us relevant results. We would also like to thank our colleagues from the Institute of Low-Carbon Industrial Processes in Cottbus for their support and feedback.

REFERENCES

[1] Fleiter, Tobias, Steinbach, Jan and Ragwitz, Mario. "Mapping and analyses of the current and future (2020-2030) heating/cooling fuel deployment (fossil/renewables): report prepared for the European Commission."

[2] Rehfeldt, Matthias, Fleiter, Tobias and Toro, Felipe. "A bottom-up estimation of the heating and cooling demand in European industry." *Energy Efficiency* Vol. 11 No. 5 (2018): pp. 1057–1082. DOI 10.1007/s12053-017-9571-y.

[3] Allen, Myles R., Opha Pauline, Dube, Solecki, William, Aragón-Durand, Fernando, Cramer, Wolfgang, Humphreys, Stephen, Kainuma, Mikiko, Kala, Jatin, Mahowald, Natalie, Mulugetta, Yacob, Perez, Rosa, Wairiu, Morgan and Zickfeld, Kirsten. "Global Warming of 1.5°C. An IPCC Special Report on the impacts of global warming of 1.5°C above pre-industrial levels and related

global greenhouse gas emission pathways, in the context of strengthening the global response to the threat of climate change, sustainable development, and efforts to eradicate poverty." URL https://www.ipcc.ch/sr15/.

[4] Arpagaus, Cordin, Bless, Frédéric, Uhlmann, Michael, Schiffmann, Jürg and Bertsch, Stefan S. "High temperature heat pumps: Market overview, state of the art, research status, refrigerants, and application potentials." *Energy* Vol. 152 (2018): pp. 985–1010. DOI 10.1016/j.energy.2018.03.166.

[5] Zühlsdorf, Benjamin, Bühler, Fabian, Bantle, Michael and Elmegaard, Brian. "Analysis of technologies and potentials for heat pump-based process heat supply above 150 °C." *Energy Conversion and Management: X* Vol. 2 (2019): p. 100011. DOI 10.1016/j.ecmx.2019.100011.

[6] McTigue, Joshua D., White, Alexander J. and Markides, Christos N. "Parametric studies and optimisation of pumped thermal electricity storage." *Applied Energy* Vol. 137 (2015): pp. 800–811. DOI 10.1016/j.apenergy.2014.08.039.

[7] Desrues, Tristan, Ruer, Jacques, Marty, Philippe and Fourmigué, Jean-François. "A thermal energy storage process for large scale electric applications." *Applied Thermal Engineering* Vol. 30 No. 5 (2010): pp. 425–432. DOI 10.1016/j.applthermaleng.2009.10.002.

[8] The Modelica Association. "Modelica." (2021). Accessed 30.11.2021, URL https://modelica.org/.

[9] Thermal Energy System Specialists, LLC. "TRNSYS: Transient System Simulation Tool." (2019). Accessed 21.12.2021, URL http://www.trnsys.com/.

[10] Gamma Technologies. "GT-SUITE Overview: From Concept Design to Detailed System Analysis." (2021). Accessed 21.12.2021, URL https://www.gtisoft.com/gt-suite/gt-suite-overview/.

[11] Mauger, Gedeon, Tauveron, Nicolas, Bentivoglio, Fabrice and Ruby, Alain. "On the dynamic modeling of Brayton cycle power conversion systems with the CATHARE-3 code." *Energy* Vol. 168 (2019): pp. 1002–1016.

[12] Marchionni, Matteo, Bianchi, Giuseppe and Tassou, Savvas A. "Transient analysis and control of a heat to power conversion unit based on a simple regenerative supercritical CO2 Joule-Brayton cycle." *Applied Thermal Engineering* Vol. 183 (2021): p. 116214. DOI 10.1016/j.applthermaleng.2020.116214.

[13] Casella, Francesco and Leva, Alberto. "Modelica open library for power plant simulation: design and experimental validation." Fritzson, Peter (ed.). *Proceedings of the 3rd International Modelica Conference* (2003).

[14] Zimmer, Dirk, Weber, Niels and Meißner, Michael. "The DLR ThermoFluidStream Library." *Proceedings of 14th Modelica Conference 2021, Linköping, Sweden, September 20-24, 2021*: pp. 225–234. 2021. Linköping University Electronic Press. DOI 10.3384/ecp21181225.

[15] El Hefni, Baligh, Bouskela, Daniel and Lebreton, Grégory. "Dynamic modelling of a combined cycle power plant with ThermoSysPro." *Proceedings from the 8th International Modelica Conference, Technical Univeristy, Dresden, Germany*: pp. 365–375. 2011. Linköping University Electronic Press. DOI 10.3384/ecp11063365.

[16] Casella, Francesco and Pretolani, Francesco. "Fast Start-up of a Combined-Cycle Power Plant: A Simulation Study with Modelica." The Modelica Association (ed.). *Proceedings of 5th International Modelica Conference*. 2006.

[17] Meinke, Sebastian, Gottelt, Freidrich, Müller, Martin and Hassel, Egon. "Modeling of coal-fired power units with thermopower focussing on start-up process." *Proceedings of the 8th International Modelica Conference; March 20th-22nd; Technical University; Dresden; Germany*: pp. 353–364. 2011.

[18] Kröger, Georg, Siller, Ulrich, Moser, Tim and Hediger, Stani. "Towards a Highly Efficient Small Scale Turboshaft Engine: Part I — Engine Concept and Compressor Design." *Volume 2B: Turbomachinery*. 06162014. American Society of Mechanical Engineers. DOI 10.1115/GT2014-26368.

[19] Oehler, Johannes, Gollasch, Jens, Tran, A. Phong and Nicke, Eberhard. "Part Load Capability of a High Temperature Heat Pump with Reversed Brayton Cycle." International Energy Agency (ed.). *13th IEA Heat Pump Conference 2021 (HPC2020) Conference Proceedings*. 2021.

[20] ESI Group. "SimulationX: Design and Analyze Your Multi-Physics System with Simulation Software." (2022). Accessed 15.02.2022, URL https://www.esi-group.com/products/system-simulation.

[21] Hindmarsh, Alan C., Brown, Peter N., Grant, Keith E., Lee, Steven L., Serban, Radu, Shumaker, Dan E. and Woodward, Carol S. "SUNDIALS: Suite of Nonlinear and Differential/Algebraic Equation Solvers." *ACM Transactions on Mathematical Software* Vol. 31 No. 3 (2005): pp. 363–396. DOI 10.1145/1089014.1089020.